I²MTC 2008 – IEEE International Instrumentation and
Measurement Technology Conference
Victoria, Vancouver Island, Canada, May 12-15, 2008

An Experimental UWB Distance Measurement System

A. De Angelis, M. Dionigi, A. Moschitta, R. Giglietti, P. Carbone
Department of Electronic and Information Engineering, University of Perugia,
via G. Duranti, 93 – 06125 Perugia, Italy.
Phone: +39 075 5853635, Fax: +39 075 5853654
E-mail: {deangelis, dionigi, moschitta, carbone}@diei.unipg.it; rikgiglio@gmail.com

Abstract *– This paper presents a distance-measuring system based on the accurate round-trip time-of-flight measurement of single Ultra-Wideband pulses, propagating between two transceiver devices. The architectures of two realized devices, referred to as master and slave, are described. The master device implements the time-interval measuring function, by means of a Time-to-Digital Converter integrated circuit, while the slave acts as pulse repeater. Both devices are designed for low-cost realization and low-power operations. This paper also presents and discusses some experimental results obtained from the system prototype. Finally, some numerical simulations results are shown, which could provide an explanation for the non-idealities in the observed distance-measuring behaviour of the system.*

Keywords *– ultra-wideband ranging, distance measurement, round-trip-time*

I. INTRODUCTION

Ultra-Wideband (UWB) technology is recently the object of considerable research and industry interest. After the 2002 FCC regulation [1], it has been proposed for next-generation high data rate wireless multimedia systems. The creation of industry associations led to a common standard platform [2] [3], based on the Multi-Band Orthogonal Frequency Division Multiplexing (OFDM) approach to UWB signal generation. However, UWB technology is also interesting for low data rate applications, in particular in the indoor positioning field. For this application, better results can be obtained using the Short-Pulse UWB technology with Time-Of-Arrival techniques [4][5][6]. By means of the fine time resolution of subnanosecond pulses, in fact, a theoretical accuracy of a few centimeters in the distance measurement can be achieved. Furthermore, this approach makes it possible to obtain other advantages, such as robustness to multipath phenomena, penetration through various types of materials, immunity to interference, low complexity and low cost [7].

This paper presents the architecture of an experimental UWB distance measuring system, based on the time-of-flight technique. Differently from the pulse-train frequency approach described in [6], in this experimental system the single pulse Round-Trip-Time (RTT) between two pulse transceivers is measured. Moreover, one of the prototypes features an on-board distance measuring capability, by means of a Time-to-Digital Converter (TDC). This approach extends the functionality of the system and allows low power operations together with better accuracy. In particular, the experimental setup presented in the above reference requires an external counter, while in this system the time interval measurement procedure is fully performed by the device without the need for any external instrument. The lower power consumption is a consequence of the single pulse transmission, as opposed to the periodic pulse train signal. Furthermore, better accuracy can be obtained in this system because of the resolution of the TDC chip and its capability of measuring time intervals as short as 3.5 ns. The system design was also focused on reducing the latency of the slave device and the associated random contribution to the measurement result, with the aim to further improve accuracy.

This paper is organized as follows. Section I describes the architecture and principle of operation of the realized system, Section II presents some experimental results and Section III reports conclusions and future developments.

II. SYSTEM ARCHITECTURE

The realized system is comprised of two Short-Pulse UWB transceiver prototypes: master and slave. For both devices, a threshold detector based on a constant-current biased tunnel diode is used at the receiving section. The operation of this section is similar to that of the device described in [6]. Furthermore, various strategies have been experimentally analyzed for the pulse generator module, as discussed in [8].

The operation of the system is divided in two phases: *addressing* and *measurement*. The first phase has been introduced to support sequential distance measurement between the master and multiple slave devices. During the *addressing* phase the master device sends a coded pulse sequence. If the slave recognizes the sequence as its addressing code, it sends the same sequence back as an acknowledge message. After receiving the acknowledge message, the *measurement* phase is initiated by the master device, which programs and initializes the TDC. Then it transmits an UWB pulse, which is received and retransmitted by the slave after a known delay. The master then receives the pulse and the TDC measures the signal RTT, by measuring the time interval occurring between the transitions of its Start and Stop input signals. At the end of the mea-

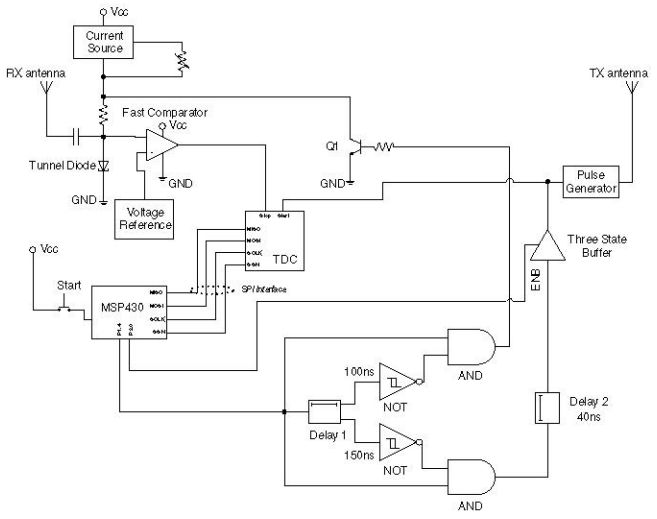

Fig. 1. Block diagram of the master device.

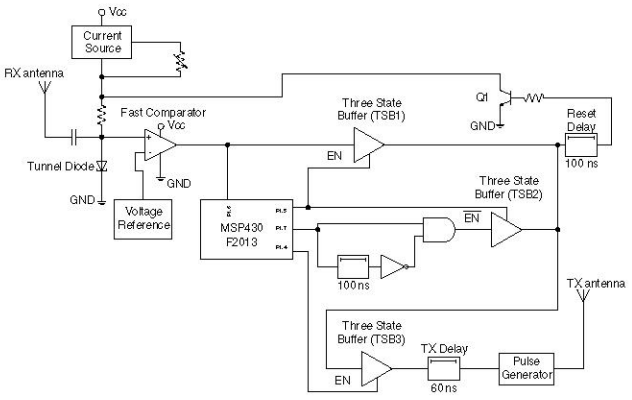

Fig. 2. Block diagram of the slave device.

surement, or repeated measurements, data stored in the flash memory of the microcontroller can be transferred to a PC.

Fig. 1 shows the block diagram of the master device. Its core component is the TDC-GP2, produced by Acam Messelectronic Gmbh, capable of measuring time intervals with a 50 ps rms resolution. The timing and control functions of the device are performed by the microcontroller, which is also used to program the TDC and to read measurement data through the Serial Peripheral Interface (SPI). The role of the delay components, realized with monolithic CMOS fixed delay lines, is to provide proper timing for the reset path of the diode (Q1 npn transistor). This prevents the tunnel diode from detecting the pulse transmitted by the same device.

Fig. 2 shows the block diagram of the slave device. Differently from the master (Fig. 1), it does not implement the measuring hardware and during the measurement phase it is only used as a pulse repeater, by enabling TSB1. During the addressing phase, instead, TSB1 is disabled and TSB2 is enabled, allowing the microcontroller to send the acknowledge message to the master.

III. EXPERIMENTAL RESULTS

The experimental characterization of the system has been conducted by placing the two devices at known distances in line-of-sight condition and processing the results of multiple RTT measurements. A Step-Recovery-Diode based pulser has been adopted [8]. Initially, simple monopole antennas have been used. Fig. 3 shows the normalized histograms of the measurement results at several distances. For each distance, apart from the last one, a standard deviation of about 0.2 ns has been observed (see Fig. 4), leading to a standard deviation of about 3 cm in the distance estimation. By performing repeated measurements, it is possible to obtain a smaller standard deviation.

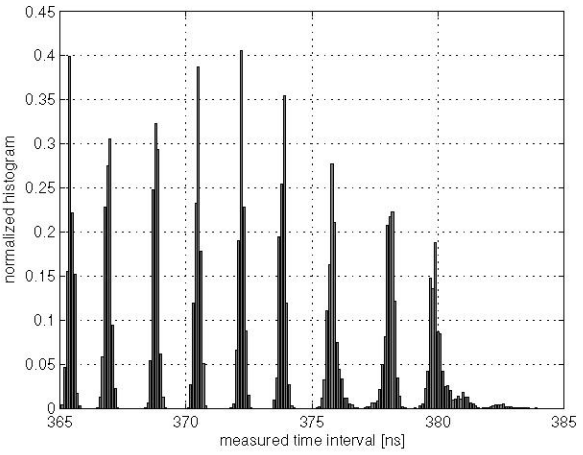

Fig. 3. Normalized histogram, 7500 RTT measurement results for each distance. Distances (left to right) from 60 to 220 cm at 20 cm steps.

Furthermore, Fig. 5 shows a plot of the mean and mode values vs distance, together with the ideal RTT values obtained by applying the formula:

$$t = \frac{2d}{c} + a, \tag{1}$$

where d is the distance, c is the speed of light in vacuum and a is a deterministic time delay introduced to compensate for the latencies of the devices.

It is worthy of notice that the measured RTT, when the distance d is increased, grows as a straight line with a higher slope than the expected one. This behaviour has been further investigated by means of simulations, performing a time domain analysis on a Gaussian pulse modulated by a sinewave, very similar to the received signal shown in Fig. 6. For instance, Fig. 7 reports several versions of a simulated received pulse, where the attenuated replicas have been obtained for different values of d, by assuming a free space path loss model. A horizontal

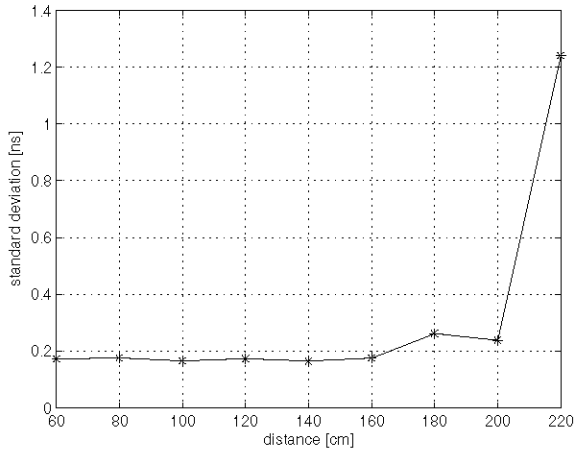

Fig. 4. Observed standard deviation of the RTT vs distance.

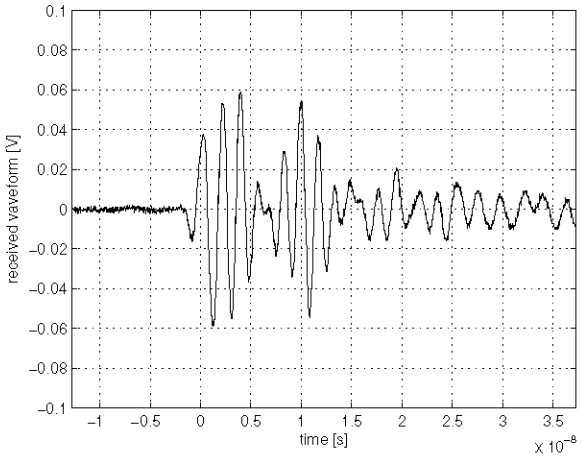

Fig. 6. Received pulse at 180 cm, 500 MHz, 1 GS/s digital oscilloscope. Monopole antenna.

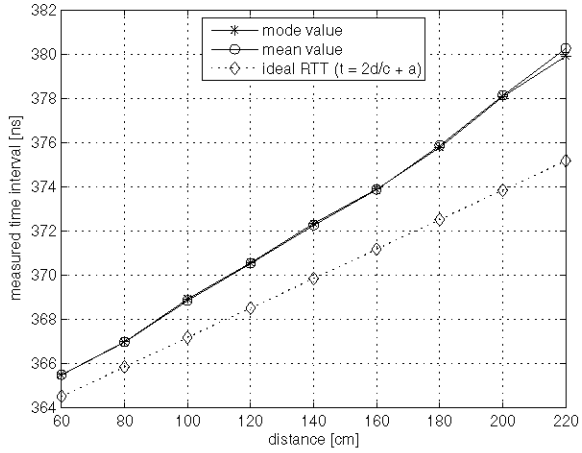

Fig. 5. Mean and mode values vs distance (continuous lines), ideal RTT vs distance (dashed line).

straight line, representing a decision threshold, is also reported. By assuming that the signal is detected as soon as the decision threshold is crossed by a positive slope portion of the signal, it can be observed that, for high values of d, the first signal peaks may be attenuated and fall below the decision threshold. Consequently, the signal detection is approximately delayed by an integer multiple of the modulating sinewave period. Moreover, a smaller delay may be added even if a signal peak does not fall below the threshold, depending on the signal slope. Thus, this phenomenon can introduce an additional delay, which behaves like a piecewise curve when d is increased. However, any sharp variations in the overall delay may not be noticeably observed in real applications, because of the smoothing effect of the various noise sources. In particular, Fig. 8 has been obtained by superimposing an Additive White Gaussian Noise to the received signal. Both the RTTs expected by considering and neglecting the AWGN contribution have been reported, together with the ideal curve

$$\begin{aligned} RTT &= \frac{2d}{c} + a, \\ a &= 2 \cdot t_0, \\ t_0 &= 0.5 \cdot 10^{-8} s, \end{aligned} \tag{2}$$

where t_0 is the approximate instant of detection of the non attenuated ideal signal, corresponding to the first significant peak in Fig. 7 exceeding the considered decision threshold. The results show a very good agreement with the experimental data of Fig. 5. Moreover, this phenomenon may also explain the behaviour shown in Fig. 3 and Fig. 4. In fact, at larger distances, the noise components could cause the detection of different peaks, resulting in a larger dispersion of the measured RTT values.

Other measurements have also been performed, with wideband discone antennas connected to the two devices. Fig. 9 shows the received signal. Notice that the signal waveform displayed is influenced by the limited scope bandwidth. In this case, however, it can be observed that the first peak of the signal is larger than the following ones. Consequently, a minor deviation from the ideal time-of-flight line is expexted. This is confirmed by the experimental RTT data of Fig. 10. In particular, the ratio between the slope of the linear regression and the slope of the ideal line for this set of data is about 1.28, while for the data in Fig. 6 it is 1.34.

Fig. 11 shows the distance measured by the master device according to the formula:

$$\hat{d} = \frac{(RTT - a) \cdot c}{2}, \tag{3}$$

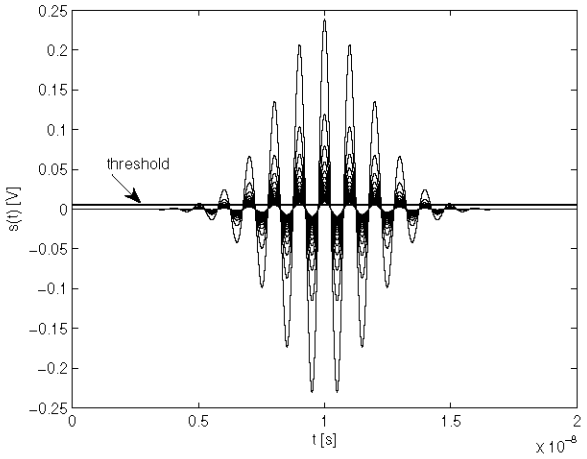

Fig. 7. Attenuated replicas of simulated received pulse and constant-value positive threshold.

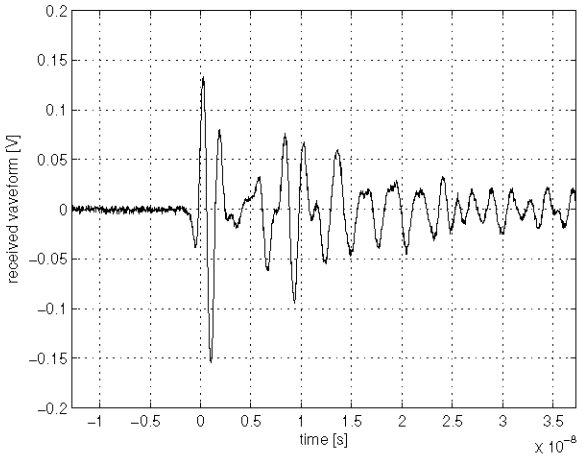

Fig. 9. Received pulse at 170 cm, 500 MHz, 1 GS/s digital oscilloscope. Discone antenna.

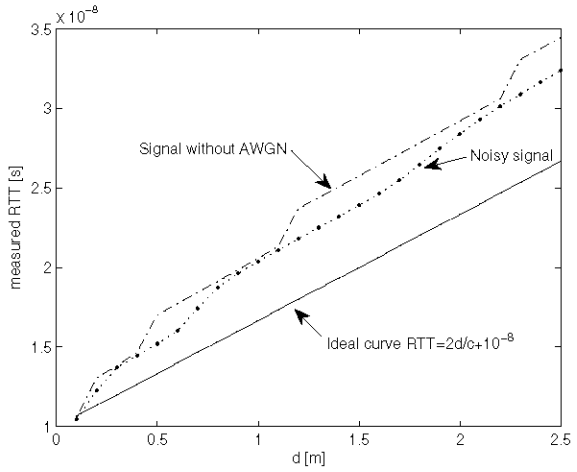

Fig. 8. Ideal RTT vs distance (continuous line), delayed detection due to the peaks of the modulating sinusoid (dots) and delayed detection in the presence of noise (dash-dot line).

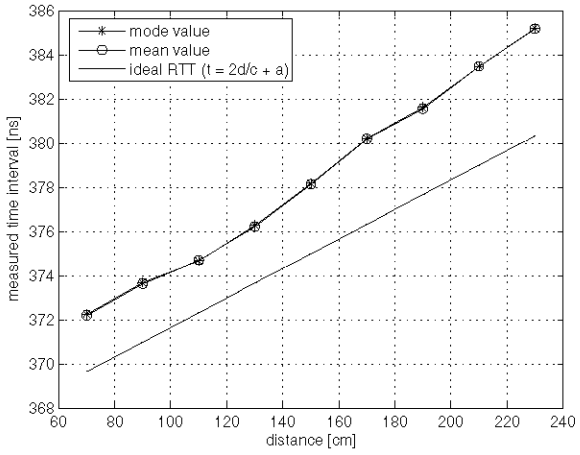

Fig. 10. Mean and mode values vs distance (continuous lines), ideal RTT vs distance (dashed line).

along with the deviation from the ideal value (actual distance). By applying linear regression to the experimental data, a correction factor has been derived. Fig. 12 shows the estimated distance after the correction. This method leads to an absolute deviation of under 8 cm and a relative deviation of under 6%.

IV. CONCLUSIONS

In this paper, an UWB distance-measuring system has been presented by describing its architecture and principle of operation. Furthermore, the main differences of the current design compared to the pulse-train frequency technique presented in [6] have been described. Experimental results have been shown and interpreted, also with the aid of numerical simulations. Future developments include the study of different receiver sections based on energy detection and correlation techniques, with the aim to extend the operating range of the system. Furthermore, a future activity is the design and experimental testing of an indoor geolocation system based on the round-trip time-of-flight technology developed so far.

References

[1] "Revision of Part 15 of the Commission's Rules Regarding Ultra-Wideband Transmission Systems," Report and order, February 14, 2002.

[2] Standard ECMA-368, *High Rate Ultra Wideband PHY and MAC Standard*, December 2005.

[3] Standard ECMA-369, *MAC-PHY Interface for ECMA-368*, December 2005.

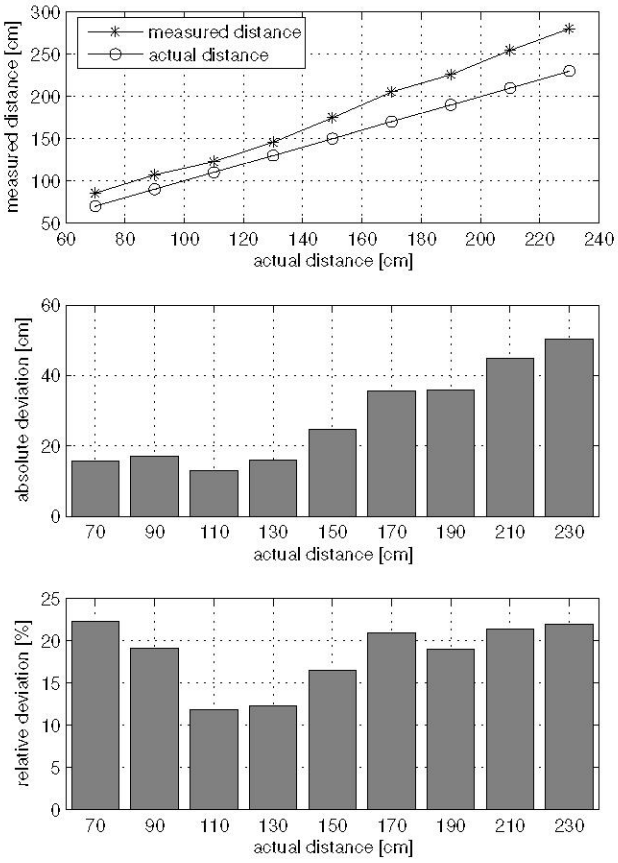

Fig. 11. Measured distance values vs actual distance, without correction.

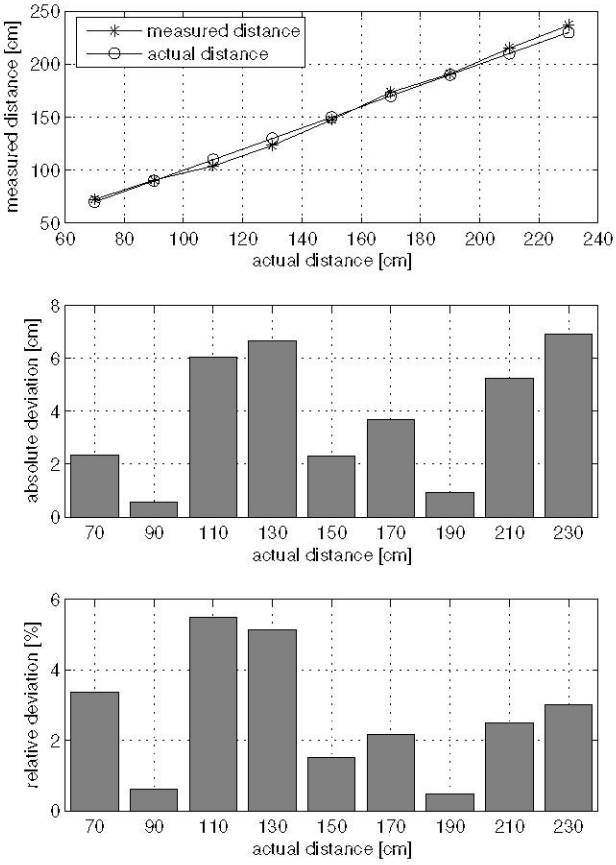

Fig. 12. Measured distance values vs actual distance, with correction based on the experimental data.

[4] S. Gezici, Z. Tian, G. B. Giannakis, H. Kobayashi, A. F. Molisch, H. V. Poor, and Z. Sahinoglu, "Localization via Ultra-Wideband Radios. A Look at Positioning Aspects for Future Sensor Networks," *IEEE Sig. Proc. Magazine*, July 2005, pp.70-84.

[5] R. J. Fontana, "Recent System Applications Of Short-Pulse Ultra-Wideband Technology," *IEEE Trans. Microw. Theory Tech.*, Vol. 52, No. 9, September 2004, pp. 2087 - 2104.

[6] A. De Angelis, M. Dionigi, A. Moschitta, P. Carbone, "A Low-Cost Ultra-Wideband Indoor Ranging Technique," *IMTC 2007 - IEEE Instrumentation and Measurement Technology Conference* Warsaw, Poland, May 1-3, 2007.

[7] A. F. Molisch, "Ultrawideband Propagation Channels – Theory, Measurement and Modeling," *IEEE Transactions on Vehicular Technology*, Vol. 54, No. 5, September 2005, pp. 1528 - 1545.

[8] A. De Angelis, M. Dionigi, R. Giglietti, P.Carbone, "Experimental Low-Cost UWB Pulse Generators," *I²MTC 2008 - IEEE International Instrumentation and Measurement Technology Conference* Victoria, Vancouver Island, British Columbia, Canada, May 12-15, 2008.